PROTEINS: Structure, Function, and Bioinformatics 65:877–888 (2006)

Aggregating the Amyloid $A\beta_{11-25}$ Peptide into a Four-Stranded β-Sheet Structure

Geneviève Boucher,[1] Normand Mousseau,[2]* and Philippe Derreumaux[3]
[1]*Département de Physique and Centre Robert-Cedergren en bioinformatique, Université de Montréal, C.P. 6128, Succursale Centre-ville Montréal, Québec H3C 3J7, Canada*
[2]*Département de Physique and Centre Robert-Cedergren en bioinformatique, Université de Montréal, C.P. 6128, Succursale Centre-ville Montréal, Québec H3C 3J7, Canada*
[3]*Laboratoire de Biochimie Théorique, UPR 9080 CNRS, Institut de Biologie Physico-Chimique et Université de Paris 7, 13 rue Pierre et Marie Curie, 75005 Paris, France*

ABSTRACT **We present a detailed analysis of the structural properties of one monomer of $A\beta_{11-25}$ as well as of the aggregation mechanisms for four chains of $A\beta_{11-25}$ using the activation–relaxation technique coupled with a generic energy potential. Starting from a random distribution of these four chains, we find that the system assembles rapidly into a random globular state that evolves into three- and four-stranded antiparallel β-sheets. The aggregation process is considerably accelerated by the presence of preformed dimers. We also find that the reptation mechanism already identified in shorter peptides plays a significant role here in allowing the structure to reorganize without having to fully dissociate. Proteins 2006;65:877–888.**

Key words: protein aggregation; Alzheimer; beta amyloid; fibrils; molecular dynamics; activation-relaxation technique; simulation

INTRODUCTION

Amyloid fibrils are insoluble self-assembled filaments formed spontaneously by a wide variety of proteins. These structures, sharing a cross β-sheet motif, have been associated with a number of important diseases (collectively referred as amyloidosis) such as Alzheimer's disease, type II diabetes, and spongiform encephalopaties.[1] Moreover, it is known that proteins can also form amyloid structures under denaturing conditions in vitro.[2,3] This common ability suggests that fibrillogenesis is a generic property of all polypeptidic chains.[3]

Fibrillar assembly has been described by the nucleation–polymerization model[4] that asserts that the formation of a stable nucleus is the rate-limiting step of the process. This is observed in vitro by a lag phase where soluble intermediates are in equilibrium prior to the rapid fibril growth.[5] Moreover, mounting evidences suggest that the toxicity observed in amyloidosis is not related to amyloid fibrils themselves but rather to the soluble intermediate oligomers formed in the early steps of fibrillogenesis.[6–8] This underlines the importance of understanding the early events inducing the assembly of misfolded peptides at the atomic level in an attempt to fight the diseases. A better characterization of these soluble intermediates would also allow a more efficient design of new inhibitors.

Amyloid fibrils and oligomers are difficult systems to study experimentally.[9] Thus, computational methods constitute a useful alternative to study the assembly of amyloid peptides. Already, computer simulations aimed at understanding the formation process and stability of various oligomeric sizes have produced of wealth of information that is now being verified experimentally.[10] These include methods such as molecular dynamics (MD),[11–17] discontinued MD,[18–20] and ART-OPEP.[21–25]

In this work, we use the activation–relaxation technique[26–29] (ART nouveau) in combination with the optimized potential for efficient structure prediction[30,31] (OPEP) to study the aggregation process of a 15-residue fragment of the β-amyloid peptide, $A\beta_{11-25}$, of sequence EVHHQKLVFFAEDVG. This fragment is known to form well-organized amyloid fibrils in vitro, similar to the pathogenic ones found in amyloidosis. Nuclear magnetic resonance (NMR) and X-ray fiber diffraction studies show that $A\beta_{11-25}$ peptides adopt an antiparallel arrangement within the fibrils[32,33] and fluorescence resonance energy transfer experiments show that the $A\beta_{11-25}$ peptides undergo multistep conformational changes (random coil, collapsed coil, micellar structure, extended β-sheet structures) in the course of the assembly process.[34] Recently, our group has described the assembly process of $A\beta_{16-22}$ dimers[21] and trimers[22] and KFFE tetramers,[23] hexamers,[25] and octamers[24] using ART-OPEP simulations. Here, we extend our investigation by studying the formation of a tetramer of $A\beta_{11-25}$.

Grant sponsors: National Sciences and Engineering Research Council (NSERC, Canada); Fonds Québécois de la recherche sur la nature et les technologies (FQRNT, Quebec); Canada Research Chair Program; Alzheimer Society of Canada.

*Correspondence to: Normand Mousseau, Département de Physique and Centre Robert-Cedergren en bioinformatique, Université de Montréal, C.P. 6128, Succursale Centre-ville Montréal, Québec H3C 3J7, Canada. E-mail: normand.mousseau@umontreal.ca

Received 10 January 2006; Revised 15 June 2006; Accepted 16 June 2006

Published online 3 October 2006 in Wiley InterScience (www.interscience.wiley.com). DOI: 10.1002/prot.21134

METHODS

ART-OPEP Simulations

The activation–relaxation technique[26,27,35] (ART) is a generic method to explore the landscape of continuous energy functions through a series of activated steps. ART events are defined directly on the energy landscape that allows the method to generate moves of any complexity. In the current implementation (ART nouveau),[27–29] one ART event consists of four steps. First, the conformation is pushed outside the minimum in a random direction until a negative eigenvalue is found in the Hessian matrix. Second, the conformation is pushed along the direction of the associated eigenvector until the total force is close to zero (indicating the presence of a first order saddle-point). Then, the conformation is slightly pushed over the saddle-point and is relaxed to a new minimum using standard minimization technique. Finally, the new conformation is accepted or rejected using a Metropolis criterion based on the energy difference between the final and initial minima ($p_{\text{accept}} = \exp(-\Delta E/k_{\text{B}}T)$). ART has the advantage of not being biased toward predetermined mechanisms and, as discussed in previous work,[28,29,36] it generates well-controlled and fully connected trajectories.

ART is used in combination with the energy model OPEP[30,31] that implements an off-lattice representation where each amino acid is represented by its N, H, C, C, O backbone atoms and each side chain is modeled by one bead with an appropriate Van der Waals radius and geometry with respect to the main chain and hydrophobic/hydrophilic character. The OPEP energy function includes four types of interactions: harmonic potentials for maintaining the stereochemical properties of the peptides, excluded-volume potential between the particles, backbone two-body and four-body hydrogen bonding interactions, and pairwise potential between sidechains considering all 20 residues identities. The N and C termini of $A\beta_{11-25}$ peptides (EVHHQKLVFFAEDVG) are neutralized using acetyl and amine groups, respectively.

As is described in more details in Ref. 29, ART-OPEP does not have detailed balance as the bias in selecting specific saddle points is unknown. Since we do not identify all the transition states of the system, it is not possible either, in general, to define a specific time scale associated with these moves. However, because the algorithm hops from energy minimum to energy minimum going through a common transition state, each generated trajectory is physically possible. Comparing ART-OPEP folding and aggregation trajectories with MD, when possible, moreover, we found a good overlap between those, showing that the trajectories generated by ART-OPEP are also physically relevant.[29]

All-Atom MD Simulation in Explicit Solvent

In addition to using ART-OPEP, we examine the stability of the four-stranded antiparallel β-sheet using MD. These are executed at neutral pH using the GROMACS[37,38] package and the all-atom force field GROMOS96.[39] The antiparallel tetramer is solvated in an octahedral box containing 12,056 water molecules and 8 Na ions, added to neutralized the peptide. MD simulations are performed with periodic conditions at a constant temperature of 330 K (which corresponds to the temperature used to grow the fibrils in vitro) and constant pressure of 1.0 atm. Bond lengths are constrained with the SHAKE algorithm[40] and the time step is set to 2 fs. Finally, the particle mesh Ewald method,[41] with a cut-off of 9.0 Å, is used to compute electrostatic forces. Graphics are obtained using the PYMOL package.[42] The secondary structure of all ART/MD generated structures was determined using the DSSP program.[43]

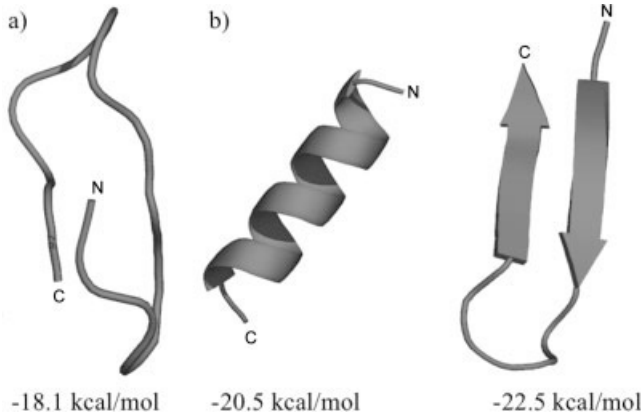

Fig. 1. Minimum-energy conformations of the monomer of $A\beta_{11-25}$ for the (**a**) random coil, (**b**) α-helical, and (**c**) β-hairpin structures.

RESULTS

Monomer Structure

Before turning to the tetramer, we characterize the solution structure of $A\beta_{11-25}$. While there is no experimental data available for $A\beta_{11-25}$, recent circular dichroism measurements on $A\beta_{11-28}$ show that, after a 13-day incubation, random coils, α-helices, and β-sheets are present in similar proportions except in very polar environment (90% HO), where α-helices are strongly disfavored and random coils dominate, and in strongly nonpolar environment (pure 1,1,1,3,3,3-hexafluoroisopopanol), where the β-sheet is the most probable structure.[44] We can expect qualitatively similar results for $A\beta_{11-25}$.

We perform four simulations of between 15,000 and 30,000 events each at 500 K starting from two different forms: fully extended and random coil. As is discussed in detail elsewhere,[28,29] the Metropolis temperature used in ART cannot be directly compared with a real temperature as the algorithm ignores the thermal vibrational effects. T is therefore selected to ensure a proper sampling of the conformational space.

The lowest energy for each of these structures is very similar: −18.1 kcal/mol for random coils, −20.55 for α-helices, and −22.5 for asymmetric β-hairpins. These conformations, shown in Figure 1, are obtained at various stages during the simulation. For example, the α and the β minima are obtained during the same 30,000-event run,

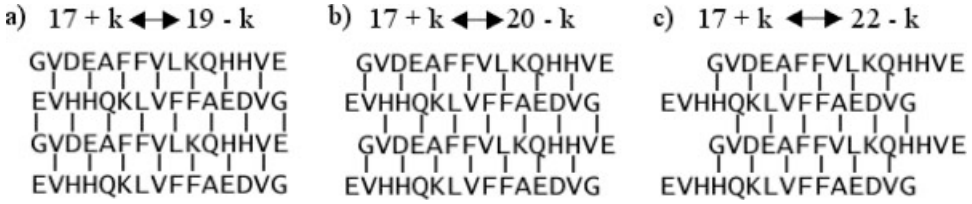

Fig. 2. Experimentally derived hydrogen bonding registries of Aβ11–25 within the fibrils. (**a**) Sikorski, (**b**) Petkova 7.4, and (**c**) Petkova 2.4. The top line indicates the short-hand nomenclature. The vertical lines below indicate the position of the intermolecular C=O···HN and NH···O=C hydrogen bonds formed.

indicating that the method ensures an extensive sampling of the conformation space of the monomer of Aβ11–25.

Because ART-OPEP does not sample the conformational space thermodynamically, it is not possible to compare our results directly with those of Juszczyk et al. for Aβ11–28. However, our results, which show that random coils, α-helices, and β-hairpins have a similar energy, agree qualitatively with the circular dichroism experiments.

Stability of β-Sheet Models

Two experimental studies[32,33] have revealed that Aβ11–25 peptides organize into fibrils with an antiparallel arrangement of the chains. From these experiments, three models have been proposed: the Sikorski model,[33] based on X-ray fiber diffraction experiments, and two models by Petkova et al.,[32] following solid-state NMR experiments executed at pH = 2.4 and pH = 7.4. These models differ mostly by the details of the hydrogen bonding registry; the Sikorski model shows a registry characterized by $17 + k \leftrightarrow 19 - k$,[33] while the Petkova 7.4 and 2.4 models have a registry of $17 + k \leftrightarrow 20 - k$ and $17 + k \leftrightarrow 22 - k$, respectively[32] (Fig. 2).

We first compare the stability of these models using ART-OPEP simulations at high temperatures. Each model is run at a series of temperatures ranging from 500 to 1500 K. At the highest temperature, which leads to a high acceptation rate (57%), a 10,000-event run fully destabilizes the Petkova 2.4 and Sikorski models, while the Petkova 7.4 model remains intact until the end. The Petkova 2.4 model reaches a fully disordered structure in less than 5000 events (3000 accepted events), whereas the Sikorski model requires an additional 2000 events to reach a disorganized state. The quick destabilization of the Petkova 2.4 model is expected as low pH conditions are not currently incorporated into OPEP. In spite of the H-bond pattern differences, both Petkova 2.4 and Sikorski models are destabilized in a similar manner: destabilization starts at the extremities of the outer strands and the fluctuations increase, breaking more and more hydrogen bonds until the whole structure collapses into a random coil.

At a Metropolis temperature of 500 and 1000 K—which should not be confused with the real temperature, as ART-OPEP moves the conformations from local minimum to local minimum, without taking the vibrational entropic contributions into account—the three models are mostly stable and only undergo some further relaxation from their initial state. For example, the Petkova 2.4 model relaxes from −169.0 to −184.2 kcal/mol, while the Sikorski and the Petkova 7.4 models relax from −184.5 and −185.2 to −197.2 and −199.0 kcal/mol, respectively.

Amongst the rearrangements observed at the lower temperatures (500 and 1000 K), we find a few occurrences of reptation movements in both the Sikorski and Petkova 2.4 models; this movement, already discussed numerically in Refs. 21 and 22, was recently confirmed by infrared spectroscopy of Aβ16–22.[10] Starting from the Sikorski model, for example, the outer strands of the tetramer change their registry to adopt the $17 + k \leftrightarrow 20 - k$ (in 3 out of 4 runs) or the $17 + k \leftrightarrow 21 - k$ (in 1 run) registry. Figure 3 shows an example of such a movement. Panel (a) presents the energy of the conformations and panel (b) indicates the total number of hydrogen bonds and show the number of new hydrogen bonds formed amongst the total with respect to the initial hydrogen bond network, at event 0. The reptation event goes as follows. Around accepted event number 600, the hydrogen-bond registry between chains 3 and 4 is disturbed, with new hydrogen bonds formed in the structure (red line in panel b), creating stored length in chain 4 (panel c, accepted event 660). All the newly formed hydrogen bonds are broken around accepted event 2200 and by event 2800 new ones are formed. The formation of these bonds corresponds to a registry $17 + k \leftrightarrow 20 - k$. Rearrangements within this new registry lead to a minimum energy structure of −193.3 at event 4385 (panel c).

Surprisingly, the reptation move has very little impact on the H-bond number (green line in panel b) and the total energy: strands 1–2 and 2–3 preserve their registry, most of strand 4 remains in contact with strand 3 and the total energy fluctuates around −185 kcal/mol and does not show any clear signature of the rearrangement taking place during the simulation. Clearly, the reptation move constitutes an elegant collective mechanism, allowing a change in hydrogen-bond registry while keeping the chains in contact.

As a complement to ART-OPEP simulations, which show a reptation move, we also examine the stability of the Sikorski model, using all-atom MD simulations with explicit water. Figure 4 presents the analysis of the 20 ns MD trajectory at 330 K. This temperature was used by Nussinov and collaborators for studying the stability of β-amyloid peptide oligomers of Aβ16–22, Aβ16–35, and Aβ10–35.[9]

During the first 5 ns, the all-atom RMSD between the initial and the MD-generated structures increases steadily to a value near 10 Å and then fluctuates around this value for the last 15 ns of the simulation. The evolution of the structure does not stop at 5 ns, however, as the radius of

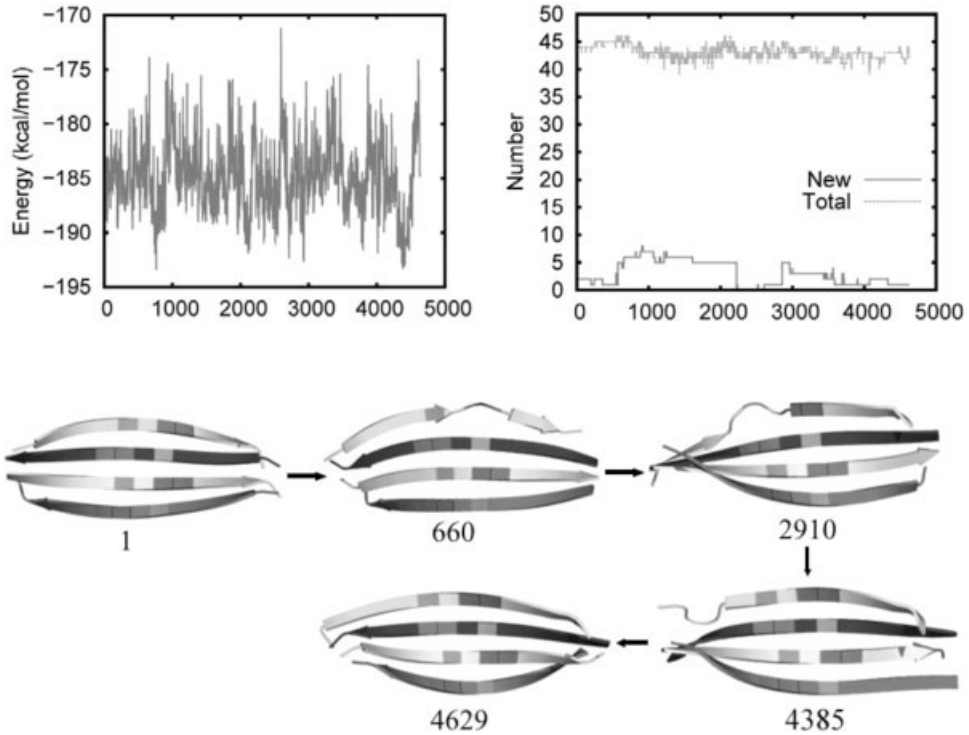

Fig. 3. The reptation movement generated by ART-OPEP starting from the Sikorski model at 500 K. (**a**) Total energy, (**b**) newly formed (bottom curve) and total (top curve) hydrogen bonds as function of the number of accepted events. (**c**) Five snapshots at events 1, 660, 2910, 4385, and 4629 illustrating the reptation move.

gyration continues to evolve during the whole simulation. We see that the number of hydrogen bonds between the main-chain atoms oscillates between 30 and 35 during most of the simulation although it decreases below 24 at 7.35 ns and quickly returns to its initial value. The changes in the number of hydrogen bonds can be correlated with the rms fluctuations observed at the extremities of the peptides, as we can see in panel (d). The core of the Sikorski model is nevertheless stable within the 20 ns simulation. As can be seen in the snapshots of Figure 4, the large fluctuations of the outer chains are associated with collective oscillations between planar and twisted conformations. This twisted deformation was already discussed in Ref. 45 for example.

Assembly From Random Initial Structures

We now turn to the characterization of the assembly process of four $A\beta_{11-25}$ chains. To characterize the early steps of aggregation, we first study the assembly process from random conformations. Following the procedure described above, we launch simulations at two Metropolis temperatures, 500 and 1000 K. At the lowest temperature, with an acceptation rate of about 30%, we run 10 independent runs counting between 10,000 and 25,000 events, starting from two initial structures with fully extended peptides randomly positioned at 10 and 20 Å, respectively, from each other; similar results are obtained starting from randomly chosen conformations of the chains.

With ART-OPEP, small peptides such as KFFE and $A\beta_{16-22}$ aggregate into a β-sheet structure within 10,000 events or less.[21,23,24] The picture is more complicated with $A\beta_{11-25}$; the four chains spend a considerable time exploring compact globular structures before organizing into β-sheets. Figure 5 shows a typical aggregation trajectory, leading to the first structure of Figure 6 (run R5). We see (panel a) that after a rapid drop in conformational energy, from −100 to −135 kcal/mol (event 3971, accepted event 1200), the relaxation process slows down as the system explores the space of conformations and finds a route to lower-energy regions. This continued exploration appears clearly in the changes of end-to-end distances. For example, around event 7195 (accepted event 2000), chain 2 stretches out from 15 to 30 Å within a few hundred events while chain 3 does the opposite at the same time, showing considerably conformation changes. As can be expected from this example, the end-to-end distance varies considerably from run to run, with values between 10 and 35 Å. Other quantities, such as the energy, the number of intermolecular hydrogen bonds and the percentage of residues adopting random coil, α-helix, and β-strand states are much more universal. Most of our simulations reach an energy between −140 and −150 kcal/mol, with about 25–30 intermolecular hydrogen bonds. Similarly, the percentage of residues in (random coil, β-strand, and α-helix) is of the order of (40, 55, and <5%).

Figure 6 shows three lowest-energy structures obtained from these independent runs. The first structure

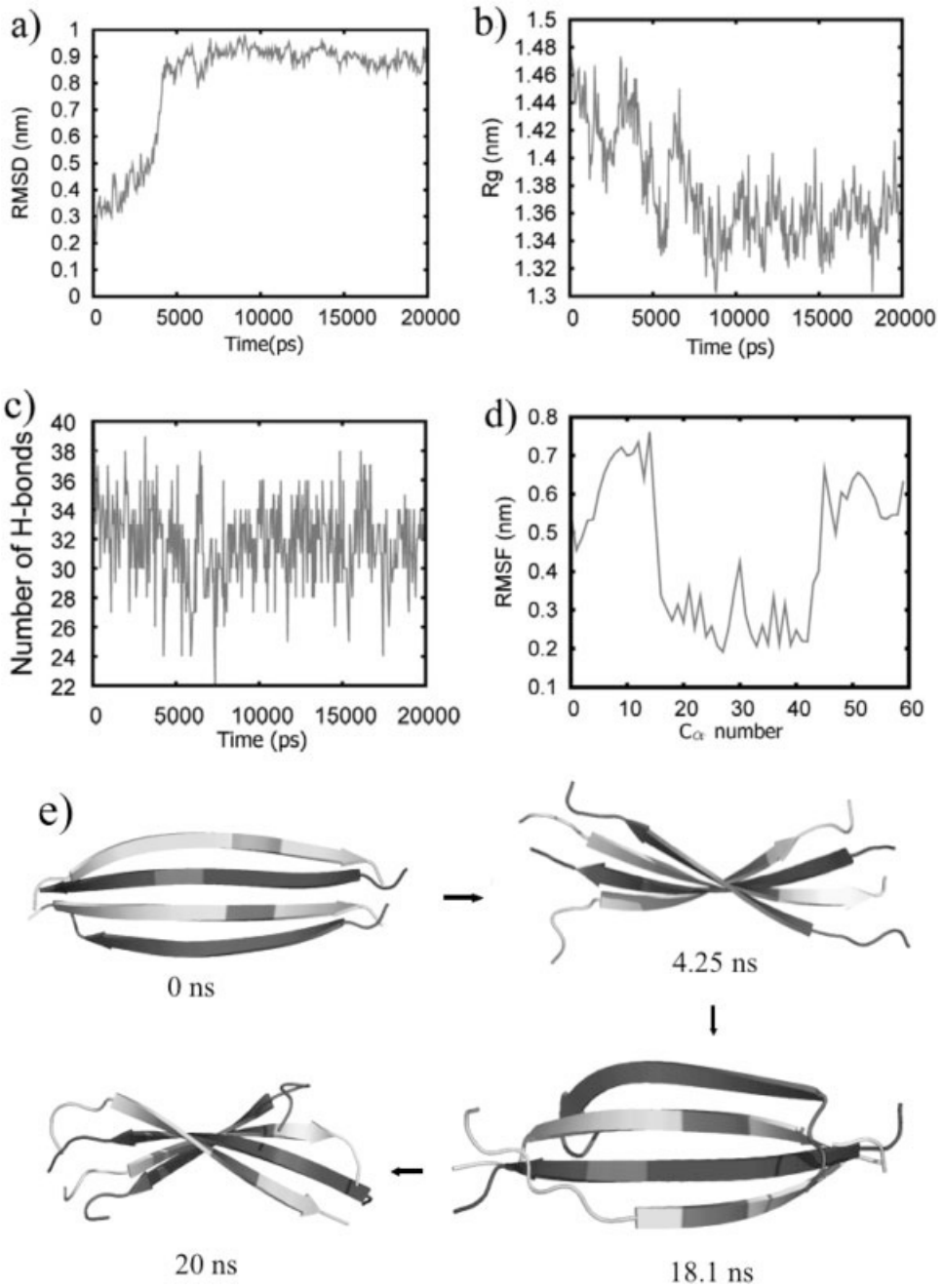

Fig. 4. Analysis of a 20 ns MD of the tetramer of $A\beta_{11-25}$ starting from the $17 + k \leftrightarrow 19 - k$ registry model proposed by Sikorsky et al. (**a**) The all-atom RMSD with respect to the Sikorski model, (**b**) the radius of gyration of the four chains, and (**c**) the number of hydrogen bonds are presented as a function of time (in ps), whereas (**d**) the time-averaged RMS fluctuation (RMSF) of C is presented as a function of the residue number (1–15 refers to chain 1, 16–30 refers to chain 2, 31–45 refers to chain 3, and 46–60 refers to chain 4). The snapshots show the structure of the tetramer at various states during the simulation.

(a) counts 31-interchain H-bonds with 58% of the residues in a β conformation and a mostly antiparallel orientation of the chains: chains 1 (red) and 2 (yellow) are stabilized by a well-formed 9-residue antiparallel β-sheet, with two additional 5-residue parallel (between chains 1 and 3 (blue)) and antiparallel β-sheets (chains 3 and 4 (green)). The second structure (b) is similarly structured with 31 interchain H-bonds, and 56% of its residues in a β conformation. The third structure (c) is less organized, with 27 interchain H-bonds and a globular-like arrangement of the chains. While the H-bond network does not show any specific preference, these three structures—especially (a) and (b)—already show a topology pointing towards the organization of β-sheets.

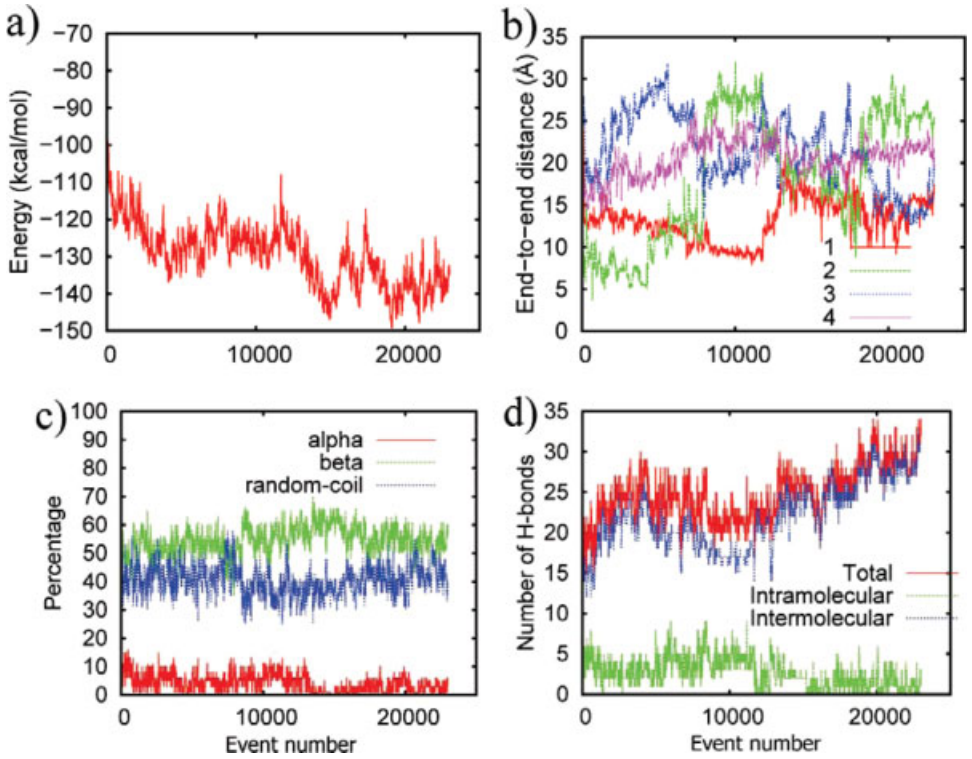

Fig. 5. Characterization of run R5, a 22,300-event ART-OPEP simulation at 500 K starting from a random conformation with four chains of $A\beta_{11-25}$ placed at distances varying between 10 and 20 Å from each other. (**a**) Energy; (**b**) end-to-end distances for every monomer; (**c**) percentage of residues in α, β, and random coil states; (**d**) hydrogen bonds: dashes, intramolecular; dotted line, intermolecular, and full line, total. All graphs are plotted as a function of event number.

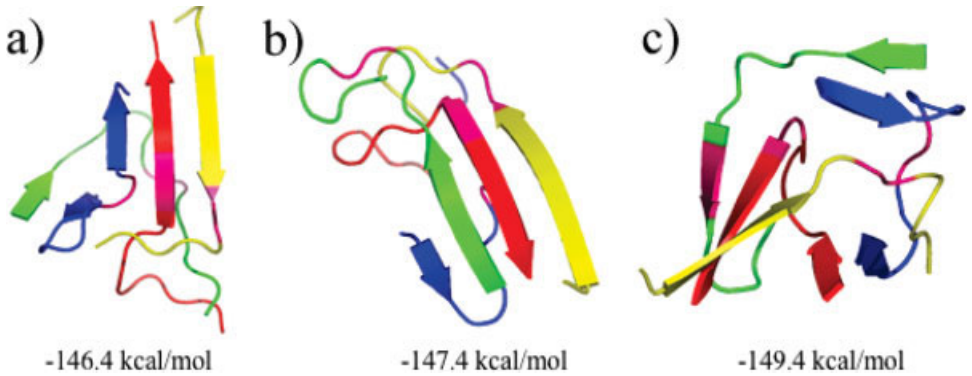

Fig. 6. Snapshots of events observed in 500 K simulations starting from a random initial structure. Snapshot (C) corresponds to run R5. Chain 1 is colored in red, chain 2 in yellow, chain 3 in blue, and chain 4 in green. Leu17 is colored in pink, Phe19 is colored in cyan, and Phe20 is in orange.

We also launch 10 runs at 1000 K. Nine out of these 10 runs collapse rapidly into disordered conformations, similar to those discussed in earlier section with an energy of −120 kcal/mol or higher. The 10th run, however, forms an ordered assembly similar to structure B in Figure 6 except that the fourth chain does not interact with the three others.

Assembly in Partially Organized Structures From Mixed Random-Preorganized Initial Structures

While four disordered $A\beta_{11-25}$ chains move towards an organized tetramer, they are still far from the fully ordered structure; significantly longer simulations would likely be necessary to fully assemble these chains. To study the last step of aggregation into an ordered four β-sheet structure, we therefore start from partially organized structures.

Because of its size and because previous simulations have underlined the importance of the dimer as a first step towards aggregation,[46,47] we study the assembly process of $A\beta_{11-25}$ starting with a preorganized dimer and either two monomers in randomly chosen conformations or a second dimer. On the basis of the results of the previous section, we use a preformed dimer with registry $17 + k \leftrightarrow 19 - k$.

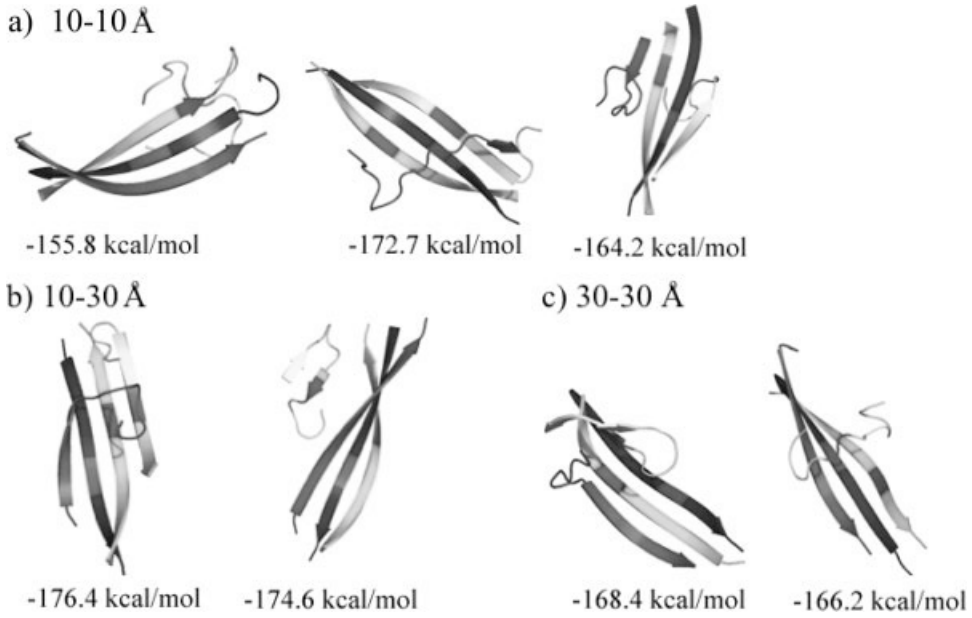

Fig. 7. Lowest-energy structures obtained from ART using the 10–10 (**a**), 10–30 (**b**), and 30–30 Å, and (**c**) preorganized initial structures.

Although organized at initial time, the two chains forming the dimer are free to move and can even break apart during the simulation that is we impose no constraint during the simulation, contrary, for example, to Ref. 13.

Aggregation of two monomers onto a preformed dimer

We first discuss simulations with a dimer and two fully stretched monomers placed perpendicularly on each side of this dimer at either 10 or 30 Å. In the initial structure called 10–10, the two monomers are at a distance of 10 Å of the dimer. In the initial structure 10–30, one monomer is positioned at 10 Å of the dimer while the other is at 30 Å away. The same logic applies to the 30–30 structure.

Each initial structure is subjected to five simulations of 10,000 events at 500 K. The energy of the most stable structures associated with the 10–10, 10–30, and 30–30 runs are between −147.6 and −158.4, −144.8 and −174.6, and −131.9 and −162.5 kcal/mol, with a mainly antiparallel orientation of the peptides. While the fluctuations are large, the results suggest that by placing one monomer further away from the ordered dimer, the system has more time to equilibrate the trimer before the fourth peptide collides, leading to lower-energy assemblies. As we see below, however, this advantage disappears once all peptides are in contact.

Counting the preformed dimer, 43% of the residues in the initial structure are in β state, with 14 already formed hydrogen bonds. The lowest-energy structures of each run possess typically between 70 and 75% of its residues in β, with about 30–32 hydrogen bonds. The most ordered structure, started from the 10–10 initial state and shown in Figure 7, has 81% of its residues in β state and 33 hydrogen bonds. These results compare well with the Petkova 7.4 model which has 88% of its residues in β state and 46 hydrogen bonds.

Ten thousand events are not sufficient for the four peptides to fully order. We thus extend the simulations by an additional 15,000 events for two 10–10 and two 30–30 runs, and an additional 5000 event for four 10–30 runs. These generate a clear energetic and structural evolution, indicating that the chains continue their move towards a more organized structures. For example, the two extended 10–10 runs converge to structures with energies 5.8 and 14.8 kcal/mol lower from their previous energy minimum, leading to conformations with an energy as low as −172.7 kcal/mol (Fig. 7). We find similar results with the 30–30 runs—with a lowest-energy structure of −168.4 corresponding to a drop of 36.5 kcal/mol with respect to the lowest-energy minimum in this given run, and the shorter 10–30 runs, with a decrease of 2.6 kcal/mol.

Figure 8 shows the detailed trajectory analysis of one of the 25,000-event simulations starting from the 10–10 state. The assembly is characterized by a decrease in the total energy of the system and by an increase in the number of intermolecular hydrogen bonds. The plots of the monomer orientation, end-to-end distance, and the number of intermolecular hydrogen bonds reveal that the preformed dimer, composed of chains 3 and 4, is stable during the whole simulation. Following the intermolecular hydrogen bonds, we see that chain 1 comes in contact with the dimer (in less than 100 events) and interacts with chains 3 and 4, whereas chain 2 interacts initially mostly with chain 1. From panel (f), which shows the respective orientation of the various pairs, we see that in the first half of the simulation, chains 1 and 2 rotate a few times, until they fall into the more favorable antiparallel orientation,

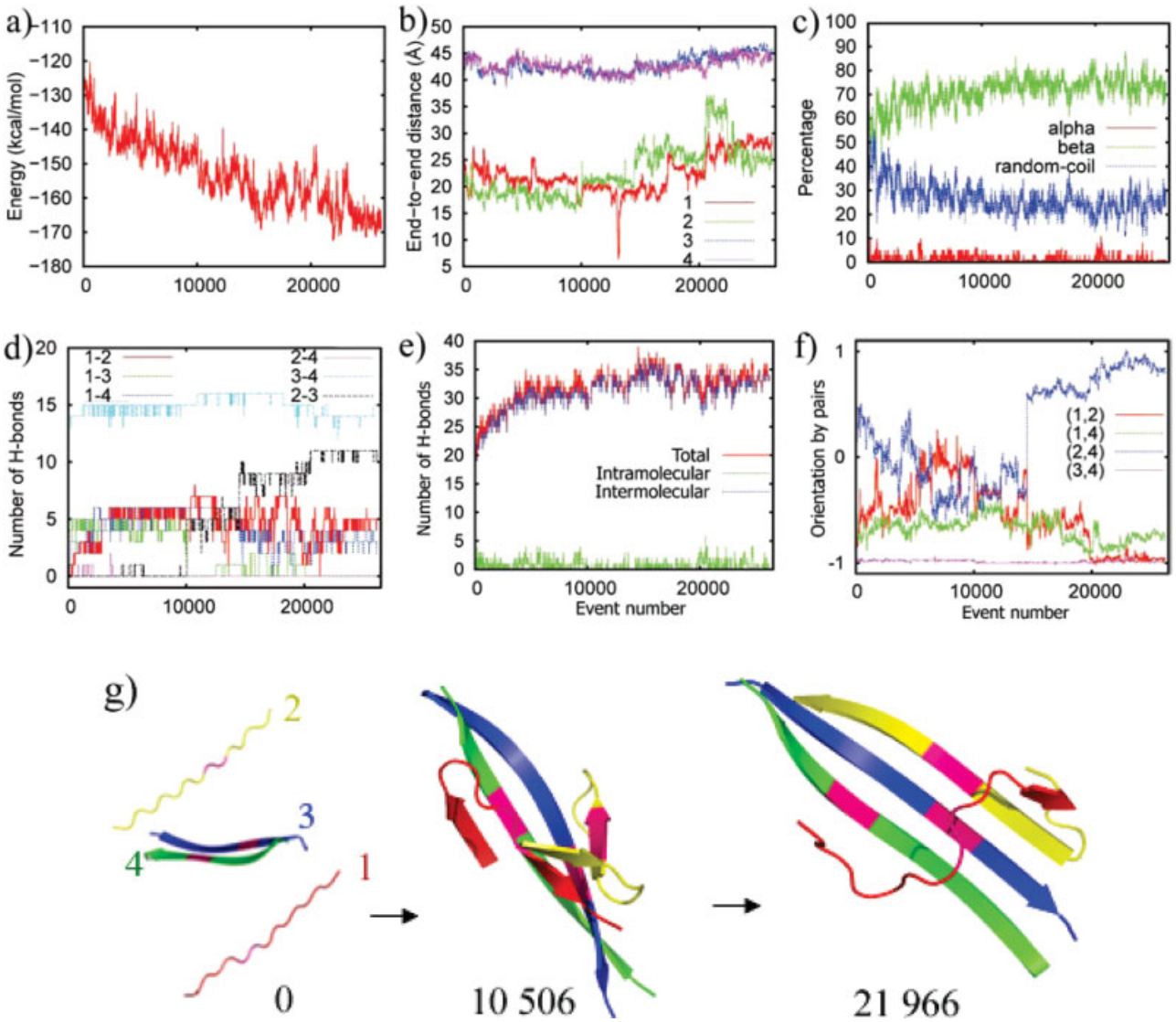

Fig. 8. Analysis of a 25,000-event run starting from the 10–10 conformation. (**a**) Total energy in kcal/mol, (**b**) end-to-end distance in Å (red = chain 1, green = chain 2, blue = chain 3, purple = chain 4), (**c**) secondary structure (green = β, red = α, blue = random-coil), (**d**) hydrogen bonds between monomers, (**e**)total number of hydrogen bonds (red = total, blue = intermolecular, green = intramolecular), and (**f**) relative orientation of the chains (1 = parallel, −1 = antiparallel) (blue = 2–4, red = 2–1, green = 1–4, purple = 3–4). All graphs are presented as a function of the event number, (**g**) Snapshots of events observed during the simulation. [Color figure can be viewed in the online issue, which is available at www.interscience.wiley.com.]

associated with a rapid increase in the number of hydrogen bonds between chain 2 and chain 3. During the last 10,000 events, chain 2 moves slightly and stabilizes itself to form a well-organized trimer with chains 3 and 4. Chain 1, which is in a conformation very similar to that of chain 2 at event 10,000, does not form a β-sheet but adopts a position stretching across the trimer and even forming short antiparallel β-sheets with both chains 2 and 4 (last snapshot, Fig. 8).

This structure, with an energy −172.7 kcal/mol, is typical of the structures obtained with this protocol. Figure 7 presents the lowest energy structures obtained starting from the three initial structures in all the simulations. The conformational energy for these structures lies between −155.8 and −176.4 kcal/mol. Except for two simulations (the third panel in (a) and second in (b)), all lowest-energy conformations show a well-formed antiparallel trimer with a monomer stretched across it. This suggests

Fig. 9. Typical mixed parallel/antiparallel tetramer observed starting from two preformed dimers.

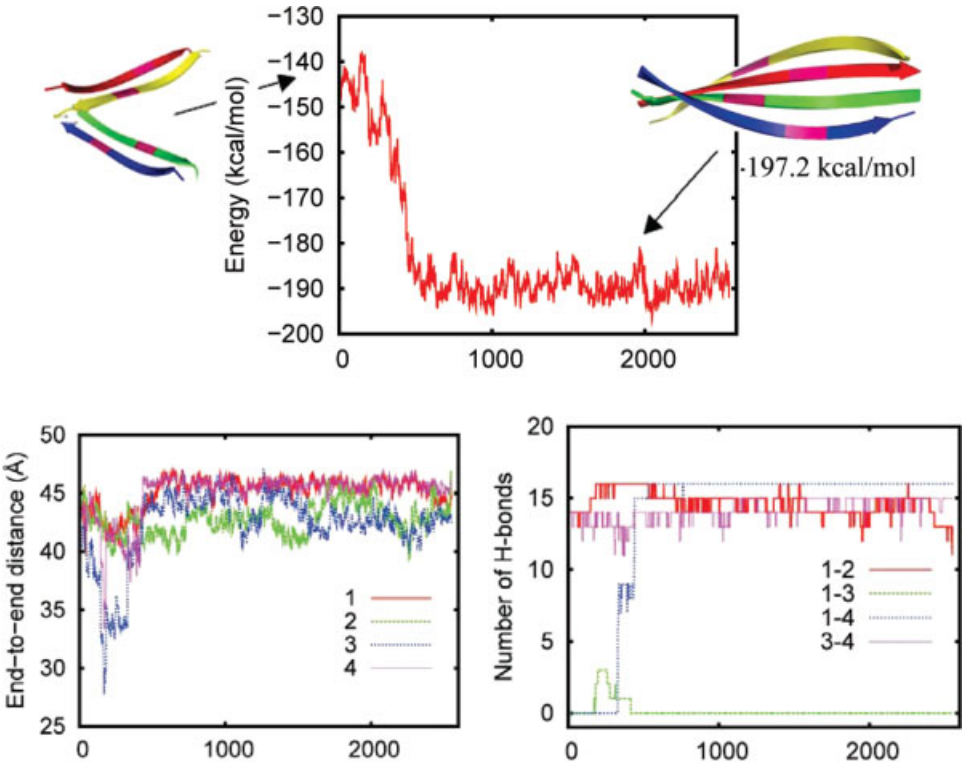

Fig. 10. Details of the aggregation process for the two preformed dimers at 500 K. The simulation analyzed here leads to an antiparallel tetramer with a minimum energy of −197.2 kcal/mol. (**a**) Total energy in kcal/mol, (**b**) end-to-end distance in Å, and (**c**) number of hydrogen bonds between monomers. Graphs are presented as a function of the number of accepted events. [Color figure can be viewed in the online issue, which is available at www.interscience.wiley.com.]

that the growth process requires stabilization of the extended structure during the first steps of assembly.

Globally, our results show that the presence of the dimer has a considerable effect on the aggregation process. Ten out of the 15 runs starting with a preformed dimer lead to an organized structure characterized by percentage of residues in β state higher than 70%; three result in the formation of an extended three-stranded β-sheet and five into structures where the four chains extend at least partly into β structures. Simulations were not sufficiently long, however, to allow the formation of fully ordered four-stranded β-sheet structures.

Aggregation of two preformed dimers

We position two copies of the antiparallel $17 + k \leftrightarrow 19 - k$ dimer in a parallel and an orthogonal orientation at a distance of 10 Å and run 8 simulations of 10,000 events each at $T = 500$ K. Since the dimers are stable at this temperature, all runs lead to extended, but imperfect, tetramers. Of these, two runs reach a fully ordered antiparallel structure corresponding to Sikorski model, one assemble into a higher-energy (−184.9 kcal/mol) mixed parallel–antiparallel four-stranded β-sheet, and five runs locate a twisted end-mixed four-stranded β-sheet (Fig. 9).

The energies of these three structures varies from −184.9 to −197.2 kcal/mol. Figure 10 shows the detailed analysis of the formation of the extended antiparallel tetramer that matches exactly the Sikorski model. We can see the stabilization of the total energy in less than 1900 events (500 accepted events). While the dimers arrange quickly into a tetramer, the end-to-end distance graph shows that the chains are not fully extended when they first collide. Rather, the chains extend as new hydrogen bonds are formed between monomers 1 and 4. Once in place, these structures, similar to the most stable organized β-sheets, are very stable.

Assembly at higher temperature

As discussed in the previous section, the aggregation process of Aβ11–25 into a four-stranded β-sheet is a slow process. Even with ART-OPEP, simulations of 25,000 events are not sufficient long to allow the complete organization to take place. To ensure that this is not a temperature effect, we also perform a number of simulations at a Metropolis temperature of 1000 K, that is, at a temperature below the destabilization point for the ordered tetramers discussed above but with a Metropolis acceptation rate between 40 and 50%, indicating a sufficient sampling of conformations.

We perform five different simulations of 10,000 events each starting from the 10–10, 10–30, and 30–30 initial structures. In most runs, the two monomers move rapidly towards to dimer, destabilize the later, and assemble into

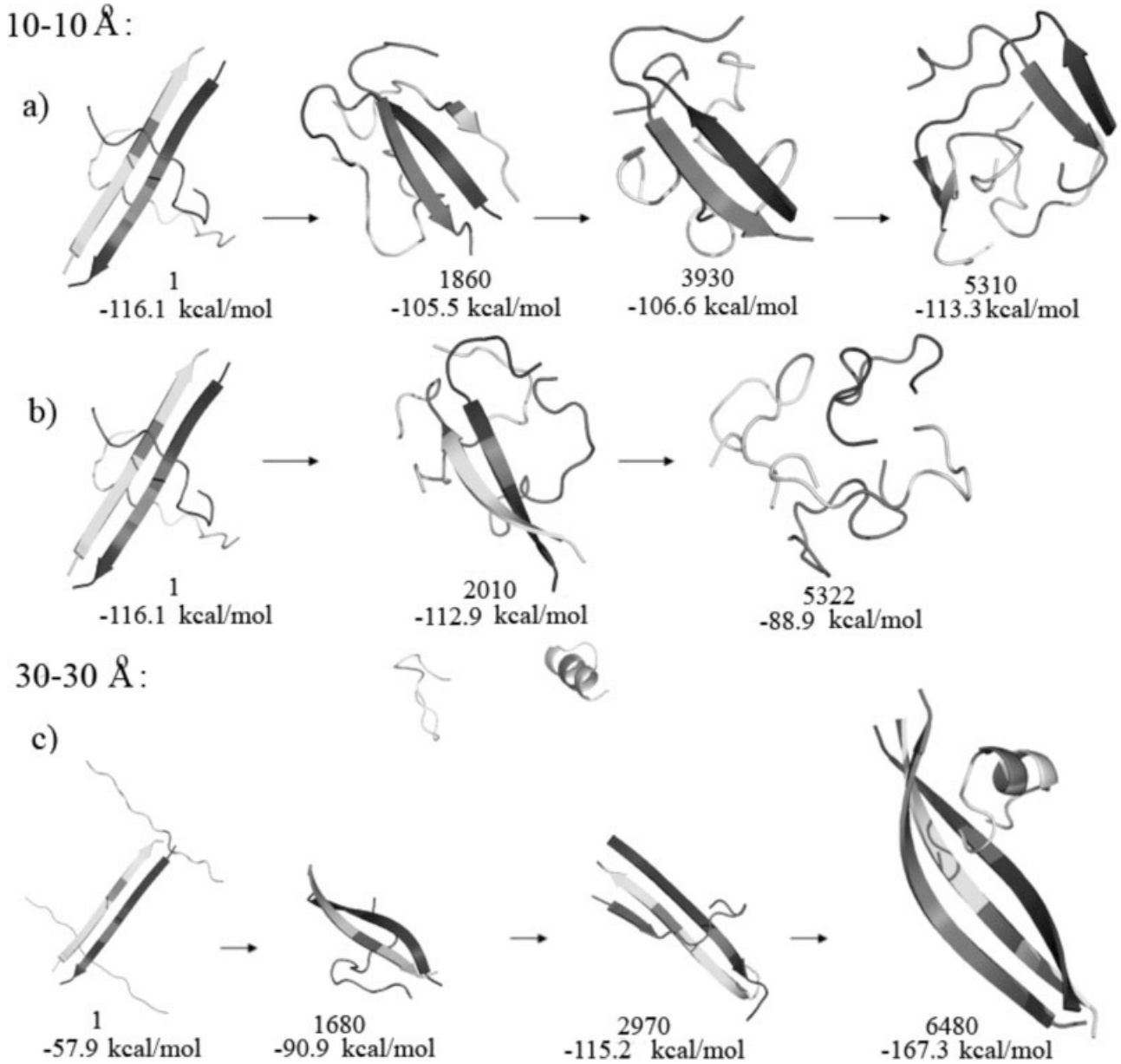

Fig. 11. Representative snapshots in 10,000-event runs at 1000 K. (**a**) and (**b**) Two runs starting from the 10–10 Å conformation and leading to overall amorphous structures. In (a), we see a significant reorganization as the initial dimer (strands 3 and 4) breaks apart and a new dimer forms partly with strands 1 and 3. (**c**) One run starting from the 30–30 Å conformation and leading to the formation of a α-helix in addition to a well-organized trimer. The helix forms early while still away from the original dimer. The numbers correspond to the accepted events.

amorphous structures [Fig. 11(b)]. In two simulations, starting from 10–10 and 30–30, we find ordered structures with a minimum energy of -167.3 kcal/mol. The assembly formed from 10–10 has 33 intermolecular hydrogen bonds and 81% of its residues are in β state. The assembly starting from 30–30 has 37 hydrogen bonds with 33 intermolecular, 76% of the residues of this system are in β state, and 11% are in α state as the fourth chain adopts a mostly monomeric α-helical structure in the second half of the simulation (event 6480) [Fig. 11(c)].

We also perform eight 10,000-event runs at the same temperature, starting from two preformed dimers places either parallel or orthogonal to each other. Five of those lead to disordered structures with partially destabilized dimers while the three other form extended tetramers, one with mixed parallel/antiparallel orientation and two with fully antiparallel orientation of the chains. Both of these fully antiparallel structures adopt the $17 + k \leftrightarrow 21 - k$ registry, with an energy of -192.7 and 194.3 kcal/mol.

DISCUSSION

In this paper, we have presented a series of simulations in an attempt to understand the first steps of aggregation

for relatively long fragments of the β-amyloid protein. The lowest-energy structure for the $A\beta_{11-25}$ monomer appears to be an asymmetric β-hairpin. However, the energy landscape has a rich set of α-helical and random coil structures competing with the lowest-energy structure near the bottom of the energy landscape. These results are consistent with circular dichroism experiments on $A\beta_{11-25}$, which also show that all three structural elements are present with the exact balance between these three types depending on the details of the environment.[44]

The role of the organized monomeric structures is minimal for the aggregation process. Placing four monomers at random in a sphere of radius 20 Å, we see that they aggregate rapidly into a globular structure, similar to what is described by Urbanc et al. in a discrete molecular dynamic simulations of $A\beta_{1-40}$ and $A\beta_{1-42}$ multimers[20] and by Colombo et al. in MD simulations of multiple replicas of the NFGAIL islet amyloid peptide.[48] Contrary to these two works, however, for most of our simulations, the disordered structures evolve relatively rapidly, showing clear evidence of trimeric or tetrameric semi-extended β-sheets within 10,000 events.

Our results, which show that it is difficult to obtain a fully extended tetramer starting with four peptides in a random conformation, are consistent with the in vivo fluorescence resonance energy transfer experiments of Kim et al.[34] In these experiments, Kim et al. found that, while $A\beta_{11-25}$ forms amyloid fibrils at high concentration, the peptides adopt micelle-like compact conformations at low concentration.

The formation of amorphous structures preceding the organization has also been seen in previous computer simulations. For example, Nguyen and Hall,[18] using discrete MD with a simplified energy potential to study the aggregation of polyalanine peptides, observe that amorphous structures systematically preceded aggregation. Similarly, Wu et al.[47] assert, based on MD results of NFGAIL peptides, that the dissociation of amorphous compact structures constitutes the limiting step of the initial process in aggregation. They suggest that hydrophobic interactions could play a key role at the beginning of the process by disfavoring organized aggregates formation.

Our results tend to support partly this suggestion. Comparing our simulations of $A\beta_{11-25}$ with the aggregation of shorter peptides such as KFFE and $A\beta_{16-22}$ in setting ranging from two to eight chains,[21,23,25] we see that the organization process seems to slow down rapidly; while 5000–10,000 events are sufficient to obtained perfectly ordered amyloid structures with the smaller peptides, 25,000 steps is not enough for the tetramer of $A\beta_{11-25}$. Nevertheless, our simulations show that $A\beta_{11-25}$ peptide can organize themselves into β-sheet-like structures without the need for an external template.

As observed previously in a number of simulations, however, the presence of a template can accelerate considerably fiber formation.[13,49,50] To explore this idea, we simulated $A\beta_{11-25}$ aggregation with one or two preformed dimers, free to disorganize during the simulation. In the first case, the four chains tend to organize into a well-formed three-stranded β-sheet with a fourth chain laying perpendicularly to the trimer. Although this last chain is unstructured, it covers the trimer and appears essential in stabilizing the trimer in its β-sheet conformation. In the second case, where two preformed dimers were placed at initial time, a four-stranded β-sheet forms in a relatively small number of events. This suggests that one of the rate-limiting step is not the dissociation of amorphous clusters, as suggested by Wu et al.[47] but the stretching of the peptides from disordered to extended states within the amorphous cluster. Once a fully extended structure is formed, aggregation should proceed rapidly.

Finally, these simulations also confirm that the dynamics of rearrangement is dominated by a reptation mechanism. By moving one strand on the other, breaking and reforming hydrogen bonds occur rapidly, in a few activate steps so that peptides do not have to detach fully from the cluster, increasing the odds of forming a lower-energy alignment. This mechanism was already predicted numerically with ART-OPEP[22,51] and Monte Carlo simulations with a simplified potential,[52] and observed experimentally[10] for smaller peptides and now seems to remain important as the peptide chain length grows.

CONCLUSIONS

In conclusion, we have presented here a detailed analysis of the aggregation mechanisms for a tetramer of $A\beta_{11-25}$ using ART-OPEP. From a random conformation, the aggregation procedure first starts in a disordered globular state that organizes itself relatively rapidly into a partially ordered β-sheet. The use of preformed ordered structure helps considerably the aggregation process, supporting the self-catalytic role of ordered oligomer in the fiber formation. Many questions remain open, however. In particular, it appears that it is difficult to form a fully organized β-sheet without the help of a surrounding cluster of other chains. This would indicate that the critical nucleus, if we count all the disorganized monomers necessary to stabilize the growing oligomer, would need to be much bigger than four. On a more fundamental basis, it would also be interesting to identify the critical length of the peptide, where process of organization goes from simple, as we see in KFFE and $A\beta_{16-22}$ to collective, as observed here. More experiments and simulations are needed to answer these central questions.

ACKNOWLEDGMENTS

The authors thank the RQCPH for generous allocation of computer times.

REFERENCES

1. Taylor JP, Hardy J, Fischbeck KH. Toxic proteins in neurodegenerative disease. Science 2002;296:1991–1995.
2. Zhao H, Tuominen EK, Kinnunen PK. Formation of amyloid fibers triggered by phosphatidylserine-containing membranes. Biochemistry 2004;43:10302–10307.
3. Stefani M, Dobson CM. Protein aggregation an aggregate toxicity: new insights into protein folding, misfolding diseases and biological evolution. J Mol Med 2003;81:678–699.

4. Harper JD, Landsbury PT. Models of amyloid seeding in Alzheimer's disease and scrapie: mechanistic thruths and physiological consequences of time dependent stability of amyloid proteins. Annu Rev Biochem 1997;66:385–407.
5. Nilsson MR. Techniques to study amyloid fibril formation *in vitro.* Methods 2004;34:151–160.
6. Kuo YM, Emmerling MR, Vigo-Pelfrey C, Kasunic TC, Kirkpatric JB, Murdoch GH, Ball MJ, Roher AE. Water-soluble aβ (n-40, n-42) oligomers in normal and Alzheimer disease brains. J Biol Chem 1996;271:4077–4081.
7. Hartley DM, Walsh DM, Ye CP, Diehl T, Vasquez S, Vassilev PM, Teplow DB, Selkoe DJ. Protofibrillar intermediates of amyloid β-protein induce acute electrophysiological changes and progressive neurotoxicity in cortical neurons. J Neurosci 1999;19:8876–8884.
8. Dahlgren KN, Manelli AM, Stine BW, Jr, Baker LK, Krafft GA, LaDu MJ. Oligomeric and fibrillar species of amyloid-β peptides differentially affect neuronal viability. J Biol Chem 2004;57:198–204.
9. Ma B, Nussinov R. Stabilities and conformations of Alzheimer's β-amyloid peptide oligomers (aβ16–22, aβ16–35, and aβ10–35): sequence effects. Proc Natl Acad Sci USA 2002;99:14126–14131.
10. Petty SA, Decatur SM. Experimental evidence for the reorganization of β-strands within aggregates of aβ(16–22) peptide. J Am Chem Soc 2005;127:13488,13489.
11. Klimov DK, Thirumalai D. Dissecting the assembly of aβ16–22 amyloid peptides into antiparallel β sheets. Structure 2003;1: 295–307.
12. Zanuy D, Ma B, Nussinov R. Short peptide amyloid organization: stabilities and conformations of the islet amyloid peptide nfgail. Biophys J 2003;84:1884–1894.
13. Paci E, Gsponer J, Salvatella X, Vendruscolo M. Molecular dynamics studies of the process of amyloid aggregation of peptide fragments of tranthyretin. J Mol Biol 2004;340:555–569.
14. Cecchini M, Rao F, Seeber M, Caflisch A. Replica exchange molecular dynamics simulations of amyloid peptide aggregation. J Chem Phys 2004;121:10748–10756.
15. Tarus B, Straub JE, Thirumalai D. Probing the initial stage of aggregation of the aβ10–35-protein: assessing the propensity for peptide dimerization. J Mol Biol 2005;345:1147–1156.
16. Lopez de la Paz M, de Mori G, Serrano, Colombo L. Sequence dependence of amyloid fibril formation: insights from molecular dynamics simulations J Mol Biol 2005;349:583–596.
17. Buchete N, Tycko R, Hummer G. Molecular dynamics simulations of Alzheimer's β-amyloid protofilaments J Mol Biol 2005; 353:804–821.
18. Nguyen HD, Hall CK. Molecular dynamics simulations of spontaneous fibril formation by random-coil peptides. Proc Natl Acad Sci USA 2004;101:16180–16185.
19. Urbanc B, Cruz L, Ding F, Sammond D, Khare S, Buldyrev SV, Stanley HE, Dokholyan NV. Molecular dynamics simulation of amyloid β dimer formation. Biophys J 2004;87:2310–2321.
20. Urbanc B, Cruz L, Buldyrev SV, Bitan F, Teplow DB, Stanley HE. In silico study of amyloid β-protein folding and oligomerization. Proc Natl Acad Sci USA 2004;101:17345–17350.
21. Santini S, Wei G-H, Mousseau N, Derreumaux P. Pathway complexity of Alzheimer's β-amyloid aβ16–22. Structure 2004;12: 1245–1255.
22. Santini S, Mousseau N, Derreumaux P. In silico assembly of Alzheimer's a peptide into β-sheets. J Am Chem Soc 2004;126: 11509–11516.
23. Melquiond A, Boucher G, Mousseau N, Derreumaux P. Following the aggregation of amyloid-forming peptides by computer simulations. J Chem Phys 2005;122:174904.
24. Wei G-H, Mousseau N, Derreumaux P. Exploring the early steps of aggregation of amyloid-forming peptide kffe. J Phys Condens Matter 2004;16:S5047–S5054.
25. Wei G-H, Mousseau N, Derreumaux P. Sampling the self-assembly pathways of kffe hexamers. Biophys 2004;87:3648–3656.
26. Barkema GT, Mousseau N. Event-based relaxation of continuous disordered systems. Phys Rev Lett 1996;77:4358.
27. Malek R, Mousseau N. Dynamics of lennard-jones clusters: a characterization of the activation-relaxation technique. Phys Rev B 2000;62:7723–7728.
28. Wei G-H, Mousseau N, Derreumaux P. Exploring the energy landscape of proteins: a characterization of the activation-relaxation technique. J Chem Phys 2002;117:11379–11387.
29. Mousseau N, Derreumaux P, Gilbert G. Navigation and analysis of the energy landscape of small proteins using the activation-relaxation technique Phys Biol 2005;2:S101–S107.
30. Derreumaux P. From polypeptide sequences to structures using Monte Carlo simulations and an optimized potential. J Chem Phys 1999;111:2301–2310.
31. Derreumaux P, Forcellino F. Computer simulations aimed at structure prediction of supersecondary motifs in proteins. Proteins 2001;45:159–166.
32. Petkova AT, Buntkowsky G, Dyda F, Leapman RD, Yau W-M, Tycko R. Solid state NMR reveals a pH-dependent antiparallel β-sheet registry in fibrils formed by a β-amyloid peptide. J Mol Biol 2004;335:247–260.
33. Sikorski P, Atkins EDT, Serpell LC. Structure and texture of fibrous crystals formed by Alzehimer's aβ(11–25) peptide fragment. Structure 2003;11:915–926.
34. Kim J, Lee M. Observation of multi-step conformation switching in β-amyloid peptide aggregation by fluorescence resonance energy transfer. Biochem Biophys Res Commun 2004;316:393–397.
35. Mousseau N, Derreumaux P, Barkema GT, Malek R. Sampling activated mechanisms in proteins with the activation-relaxation technique. J Mol Graph Model 2001;19:78–86.
36. Mousseau N, Derreumaux P. Exploring the early steps of amyloid peptide aggregation by computers. Acc Chem Res 2005;38:885–891.
37. Berendsen HJC, Van der Spoel D, Van Drunen R. Gromacs: a message-passing parallel molecular dynamics implementation. Comput Phys Commun 1995;91:43–56.
38. Lindahl E, Hess B, Van der Spoel D. Gromacs 3.0: a package for molecular simulation and trajectory analysis. J Mol Mod 1995;7: 306–317.
39. Scott WRP, Hunenberger PH, Tironi IG, Mark AE, Billeter SR, Fennen J, Torda AE, Huber T, Kruger P, Van Gunsteren WF. The gromos biomolecular simulation program package. J Phys Chem 1999;103:3596–3607.
40. Myamoto S, Kollman PA. Settle: an analytical version of the shake and rattle algorithms for rigid water models. J Comput Chem 1992;12:952–962.
41. Essman U, Perela L, Berkowitz M, Darden T, Lee H, Pedersen LG. A smooth particle mesh ewald method. J Comput Phys 1995;103: 8577–8592.
42. DeLano WL. The pymol molecular graphics system. DeLano Scientific, San Carlos, CA. Available at http://www.pymol.org, 2002.
43. Kabsch W, Sander C. Dictionary of protein secondary structure: pattern recognition of hydrogen bonded and geometrical features. Biopolymers 1983;22:2577–2637.
44. Juszczyk P, Kolodziejczyk A, Grzonka Z. Circular dichroism and aggregation studies of amyloid β (11–28) fragment and its variants. Acta Biochim Pol 2005;52:425–431.
45. Soto P, Cladera J, Mark A, Daura X. Stability of siv gp32 fusion-peptide single-layer protofibrils as monitored by molecular-dynamics simulations. Angew Chem Int Ed 2005;44:1065–1067.
46. Hwang W, Zhang S, Kamm RD, Karplus M. Kinetic control of dimer structure formation in amyloid fibrillogenesis. Proc Natl Acad Sci USA 2004;101:12916–12921.
47. Wu C, Lei H, Duan Y. The role of phe in the formation of well-ordered oligomers of amyloidogenic hexapeptide (nfgail) observed in molecular dynamics simulations with explicit solvent. Biophys J 2005;88:2897–2906.
48. Colombo G, Daidone I, Gazit E, Amadei A, Di Nola A. Molecular dynamics simulation of the aggregation of the core-recognition motif of the islet amyloid polypeptide in explicit water. Proteins 2005;59:519–527.
49. Harrison P, Chan H, Prusiner S, Cohen F. Conformational propagation with prion-like characteristics in a simple model of protein folding. Protein Sci 2001;10:819–835.
50. Dima R, Thirumalai D. Exploring protein aggregation and self-propagation using lattice models: phase diagram and kinetics. Protein Sci 2002;11:1036–1049.
51. Wei G-H, Derreumaux P, Mousseau N. Sampling the complex energy landscape of a simple β-hairpin. J Chem Phys 2003;119: 10712–10716.
52. Imamura H, Chen JZ. Dependence of folding dynamics and structural stability on the location of a hydrophobic pair in β-hairpins. Proteins 2006;63:555–570.